RSC Advances

ROYAL SOCIETY OF CHEMISTRY

www.rsc.org/advances

Journal Name

ARTICLE

A complementary electrochromic device based on $W_{18}O_{49}$ nanowire arrays and Prussian blue thin films

Received 00th January 20xx,
Accepted 00th January 20xx

DOI: 10.1039/x0xx00000x

www.rsc.org/

Chih-Hao Lu[a], Min-Hsiung Hon[a,b] Chi-Yun Kuan[c], and Ing-Chi Leu*[d]

Tungsten oxides ($W_{18}O_{49}$) nanowire arrays as effective electrochromic working electrodes were fabricated on seed-free FTO glasses through a facile solvothermal process. XRD, FESEM and TEM were used to characterize the phase, morphology and nanostructure. Uniform monoclinic $W_{18}O_{49}$ nanowire arrays can be obtained at 180°C for 5h. In the assembled electrochromic device the $W_{18}O_{49}$ nanowire array films show a fast response and switching time, extracted for a 50% transmittance change of 10.8 s for coloration (t_c) and 3.1 s for bleaching (t_b), which surpass current traditional devices using monoclinic tungsten oxide (WO_3) as the electrochromic material. The reasons can be attributed to their large specific surface area, special tunnel structure and non-stoichiometry characteristics. A complementary electrochromic device combining the $W_{18}O_{49}$ nanowire arrays with Prussian blue film shows a higher optical contrast (59.05% at 632.8nm) and a faster switching response with a coloration time of 6.9s and a bleaching time of 1.2s, superior to the single layer $W_{18}O_{49}$ nanowire device. The complementary device with excellent electrochromic performance demonstrates a great potential for practical application.

Introduction

Electrochromic materials are able to change their optical properties persistently and reversibly by a small external electrical voltage change, making them potential candidates for applications in antiglare mirrors[1,2], high contrast displays and energy-saving smart windows[3,4]. The tunable visible light transmittance resulting from the color change of the electrochromic materials are much desired in smart window devices, which not only increases the aesthetic of traditional windows but also saves energy by reducing heating or cooling loads of the building interiors. The transition metal oxides of Ti[5], V[6], Ni[7] and W[8] are widely studied for their electrochromic behavior. Among these materials, WO_3[9] is of considerable interest due to low cost, high coloration efficiency (CE) and good cyclic reversibility. Moreover, tungsten oxides, as one of the important metal oxides, are the most widely investigated materials for electrochromic devices because they can be used as intercalation host for H^{+}[10], Li^{+} and Na^{+}[11] to form tungsten bronze with blue color due to their special tunnel structure. Unfortunately, amorphous[12]tungsten oxides have poor electrochemical durability, resulting in research work to be mainly focused on nanostructured crystalline tungsten oxides. Besides, nanostructured tungsten oxide with large surface areas is expected to improve the switching response characteristics of crystalline tungsten oxide by increasing the active surface in the electrochemical process. In the past years, one dimensional tungsten oxide nanostructures with large surface areas, including nanotubes[13], nanorods[14,15,16] and nanowires[17,18], have been widely investigated. For electrochromic application, tungsten oxide nanostructures need to be synthesized as a film onto conductive substrate. In brief, two drawbacks may affect the device performance thus fabricated: (a) the poor contact between the tungsten oxide nanorods or nanowires and the transparent conductive substrate; (b) the difficulty to control the film uniformity of the deposited active materials. The nanostructures of the tungsten oxide film are found to affect the performance of the electrochromic devices, which in turn may largely depend on the film fabricating techniques and processing conditions. Such nanostructured tungsten oxides have been synthesized by sol-gel[19], sputtering[20,21], hydrothermal[22,23] and solvothermal[24] methods. Considering practical applications, high coloration efficiency and long-term stability are required for non-stoichiometric tungsten oxide films, the solvothermal approach is one of the most promising methods for fabricating tungsten oxide films because of its advantages of low cost, simple operation and inexpensive apparatus. Although synthesis of $W_{18}O_{49}$ by using the solvothermal method with alcohol as the reactant has been reported [32,37], this paper focuses on how to directly synthesize non-stoichiometric $W_{18}O_{49}$ nanowires arrays onto bare FTO glass substrates.

[a]Department of Materials Science and Engineering, National Cheng Kung University, Tainan, Taiwan, Republic of China
[b]Research Center for Energy Technology and Strategy, National Cheng Kung University, Tainan, Taiwan, Republic of China
[c]Technical Department, Thintech Materials Technology Co., LTD., Kaohsiung, Taiwan, Republic of China
[d]Department of Materials Science, National University of Tainan, Tainan, Taiwan, Republic of China. E-mail: icleu@mail.mse.ncku.edu.tw

Among the various tungsten oxides, non-stoichiometric tungsten oxides (WO_{3-x}, $0<x<1$), such as WO_2[25] and $W_{18}O_{49}$[26], are attracting more interest due to their unique defects in crystalline structure. Non-stoichiometric tungsten oxides have been found to have potential application in various fields, including field emission[27], gas sensors[28] and photocatalysis[29]. Up to now, there are only few reports on the electrochromic properties of non-stoichiometric tungsten oxides. Direct synthesis of $W_{18}O_{49}$ nanowire arrays as the electrochromic film onto FTO glass were performed through a facile solvothermal method, and their electrochormic properties were investigated in this study.

Prussian blue (PB, iron (III) [hexacyanoferrate (II)]), a coordination-compounded transition metal hexacyanometallate, is a suitable complementary electrochromic material to tungsten oxide due to its outstanding electrochromic performance and proper operational voltage range. Compared with a single layer electrochromic device, it is well known that a complementary device containing two proper electrochromic layers could further improve the performance, for example, the optical contrast and coloration efficiency. Although complementary electrochromic devices with improved properties based on electrodeposited WO_3 and PB films have been reported[30], to the best of our knowledge, no work has been done on applying the solvothermally grown nanostructured non-stoichiometric tungsten oxide films in complementary electrochromic devices.

In this paper, nanowire arrays of $W_{18}O_{49}$ crystals were directly prepared on bare FTO glass via a simple solvothermal method. We describe the solvothermal growth of $W_{18}O_{49}$ nanowire arrays under varied reaction conditions. The structure, morphology and electrochromic property of the resulting nanostructured non-stoichiometric tungsten oxide films are investigated and demonstrated to be a good alternative electrochromic material. Moreover, complementary electrochromic devices combining the non-stoichiometric tungsten oxide film with PB film is fabricated and an increased optical modulation and a faster switching response are obtained.

Experimental Section

Synthesis of non-stoichiometric tungsten oxide nanowire arrays

The non-stoichiometric tungsten oxide nanowires arrays were synthesized by using a solvothermal method with tungsten hexachloride (WCl_6) as precursor and methanol as solvent. The procedures were the same as those described in our previous paper[32]. The steps are described briefly as follows. In a typical procedure to prepare non-stoichiometric tungsten oxide nanowire arrays, 0.3g WCl_6 was dissolved in 50mL of methanol in a beaker to obtain a solution. The precursor solution has been vigorously stirred for 1hr, forming a transparent precursor solution. Subsequently, the solution was transferred to a 60ml teflon-lined stainless steel autoclave. After that, pieces of FTO glass substrate were immersed into the reaction solution with an angle against the wall. Then, the autoclave was sealed and maintained at 180℃ for 0.5~5 h in an electric oven. After cooling down to room temperature naturally, the products were washed with deionized water for several times, and the obtained samples were dried at 70ºC for 2hr in air.

Electrodeposition of Prussian blue and fabrication of complementary electrochromic device

The electrodeposition of Prussian blue film was carried out by a standard two-electrode system. The transparent and conductive FTO coated glasses with dimensions of $25 \times 20 \times 1$ mm^3 were used as the the working electrode, and a platinum sheet as the counter electrode. The electrodeposition solution of Prussian blue contained 0.025M $K_3Fe(CN)_6$, 0.025M $FeCl_3$ and 0.05M K_2SO_4 and the electrodeposition process was carried out by applying a constant electrical voltage of 1V for 120 s. The thickness of the as-deposited Prussian blue film is about 400 nm (measured by an FE-SEM; Hitachi S4800). Then the $W_{18}O_{49}$ nanowire arrays as working electrode and Prussian blue thin film as the counter electrode were sealed together. An electrolyte composed of 1M lithium perchlorate ($LiClO_4$) and poly(methyl methacrylate) (PMMA) in propylene carbonate (PC) was introduced between the two electrodes by capillary action. Finally the cell was sealed with hot glue.

Characterization

The phase structure of tungsten oxide was analyzed by X-ray diffraction (XRD) using a Rigaku D/Max diffractometer in the range of 10 to 60º with Cu Kα source radiation at room temperature. A field-emission scanning electron microscope (FE-SEM; Hitachi S4800) was used for morphology characterization of the samples. Before characterization, the FESEM sample was coated by Pt film using a sputtering machine at a beam current of 20mA for 120s. The high-resolution transmission electron microscopy (HRTEM) and the selected area electron diffraction (SAED) observations were performed on a JEOL JEM-2010UHR instrument at an acceleration voltage of 200 kV.

For electrochromic device characterization, the non-stoichiometric tungsten oxide nanowire arrays were coated onto the FTO glass and acted as the working electrode and Prussian blue was deposited onto the FTO glass as the counter electrode. The transmittance spectra were measured by an UV-vis spectrophotometer (JASCO V-600) in the spectral range between 300 and 1000 nm. Finally, the coloration/bleaching switching behavior of non-stoichiometric tungsten oxide nanowires arrays on FTO glass was measured by optical transmittance change using an UV-vis spectrophotometer at the wavelength of 632.8 nm with alternately applying a square wave voltage of 2.0V to negative 2.0V, for 100s for each state.

Results and discussion

The XRD pattern indicates that highly pure crystalline $W_{18}O_{49}$ is formed without other crystal phases, as shown in fig.1 (b). It reveals a monoclinic phase in which the 2θ scan has peaks at 23.4º and 47.9º, corresponding to the (010) and (020) planes of monoclinic $W_{18}O_{49}$, respectively. The XRD result shows a stronger intensity from the (010) peak. Moreover, XRD peak intensity of the (010) plane was relatively higher than that of other planes. This implies

that the nanowires grow along the [010] direction. Lou et al.[31] has synthesized crystalline WO_{3-x} nanowire arrays by solvothermal reaction. The WO_{3-x} nanowire with strong (010) peak indicates the preferential growth of tungsten oxide along the [010] direction. Similar behaviors have been reported for

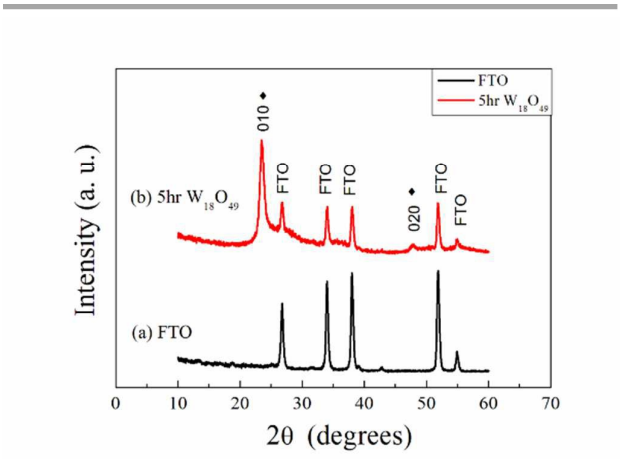

Fig.1 XRD patterns of (a) FTO substrate, (b) as-prepared $W_{18}O_{49}$ nanowire array film after the solvothermal method at 180°C for 5h.

$W_{18}O_{49}$ nanowires[31], which indicates a preferential growth along the [010] direction. The other peaks belong to the peaks of FTO substrate. In order to investigate the growth behavior of $W_{18}O_{49}$ nanowire arrays, the solvothermal synthesis process was kept at 180 ℃ for different growth time. Fig. 2 shows the various $W_{18}O_{49}$ products synthesized as a function of reaction time in this work. From fig.2 (a) FESEM image, the product of metal oxide is in the form of a smooth coating that covers uniformly on the FTO glass. When the growth time was increased to 1h, some randomly deposited tungsten oxide particles were revealed as white spots on the above-mentioned smooth coatings on the FTO glass, which is shown in fig 2 (b) FESEM image. Compared with traditional WO_3 material, $W_{18}O_{49}$ has a strong anisotropic growth behavior along the [010] direction[32]. After prolonging the growth time to 2.5h, wire-like morphology can be

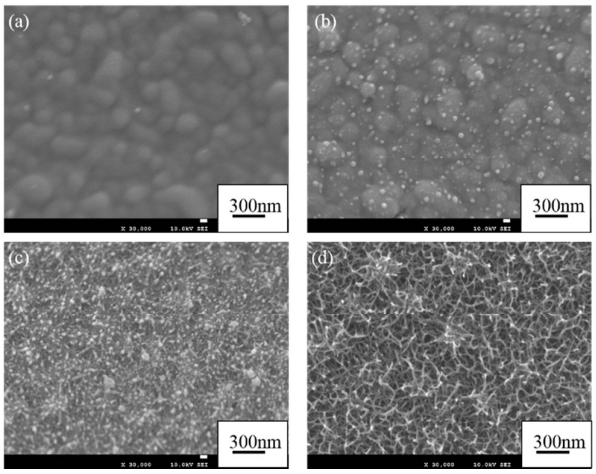

Fig.2 FESEM images of $W_{18}O_{49}$ nanowire arrays on FTO substrate via a solvothermal synthesis at 180 ℃ for (a)0.5, (b)1, (c)2.5, and (d)5 h.

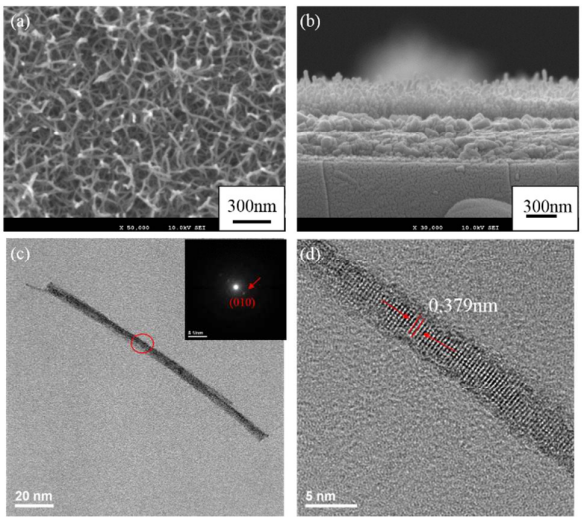

Fig. 3 (a) and (b) FESEM images of $W_{18}O_{49}$ nanowire arrays on FTO substrate. (c) TEM image and (d) High resolution TEM image of a scraped $W_{18}O_{49}$ nanowire (NBDP as an insect).

obtained and the nanowires become longer and are dispersed randomly to form the nanowire arrays.

Finally, the surface of FTO was covered by the uniform $W_{18}O_{49}$ nanowire arrays, which is shown in fig. 2 (d) FESEM image. The growth process of $W_{18}O_{49}$ nanowires may be explained as follows: The dissolution of WCl_6 in methanol leads to tungsten-containing compound precursors that are converted into tungsten oxide nuclei upon solvothermal treatment. The continuous growth of the nuclei along the [010] direction results in forming tungsten oxide nanowires.

The SEM top-view and cross-section images of the solvothermally synthesized $W_{18}O_{49}$ nanowire arrays for 5 h are shown in figure 3 (a)

and (b). The $W_{18}O_{49}$ nanowire array films exhibit a high aspect-ratio wire structure with an average diameter ranging from 6~25nm and a film height of 200~400nm. It is believed that this interwoven feature is helpful to enhance the follow-up electrochemical processes and the resulting performance of electrochromic devices. Figures 3 (c) and (d) are TEM analyses of the scraped $W_{18}O_{49}$ nanowires from FTO substrate. It can be seen that monoclinic $W_{18}O_{49}$ nanowires with an average diameter of ~6 nm are successfully synthesized. The insect of fig. 3(c) depicts the SAED pattern of the nanowire. From fig. 3(d), the lattice spacing of an individual nanowire is measured to be about 0.379nm, corresponding to the (010) plane of monoclinic $W_{18}O_{49}$. Combined with the XRD and TEM analysis, it can be realized that the individual nanowires of $W_{18}O_{49}$ should follow the same growth direction during the solvothermal reaction, i.e. [010] direction.

An electrochromic device has been fabricated with a simple two-electrode configuration for preliminary investigation. The complementary device is schematically shown in fig.4. The non-stoichiometric monoclinic $W_{18}O_{49}$ nanowire arrays were coated onto FTO glass as the working electrode. Then, the home-made gel electrolyte was spread onto the FTO glass without/with coated Prussian blue as a counter electrode.

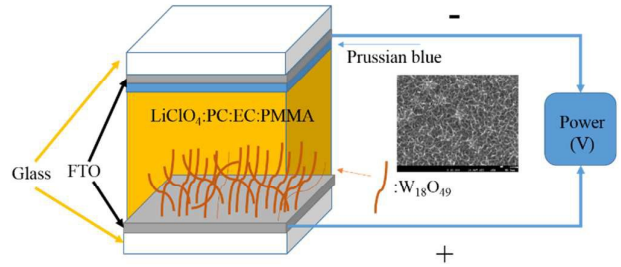

Fig.4 A schematic of complementary device with the tungsten oxide nanowire and Prussian blue as the electrochromic layer.

Finally the two electrodes with the sandwiched electrolyte in between were assembled to make both the traditional and complementary device. It is well-known that the intercalation and de-intercalation of electrons from the electrode and Li^+ ions from the electrolyte result in the bleaching and coloration processes of the tungsten oxides, which can be expressed as the following reaction:

$$W_{18}O_{49}\,(\text{bleach}) + x\,Li^{+} + x\,e^{-} \leftrightarrow Li_x W_{18}O_{49}\,(\text{blue})$$ [33]

It is worth pointing out that the as-prepared $W_{18}O_{49}$ nanowire array films grown on the FTO substrate can have high transmittance at visible light range (almost the same with bare FTO glass), which indicates that the electrochromic device also can have a high contrast performance. The device quickly displayed a blue color at -3.0 V and bleached to colorless state at +3.0 V, as shown in figure 5 (a,b). The colored $W_{18}O_{49}$ film can retain its colors for several days after the applied voltages were removed.

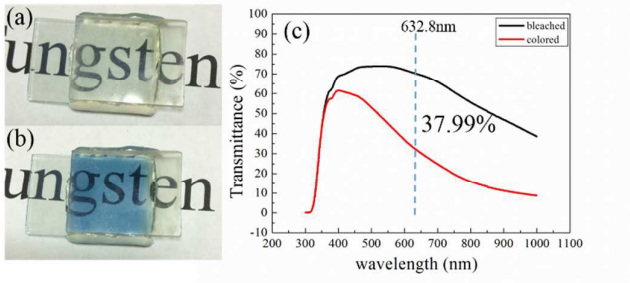

Fig.5 (a) Photograph of bleached state electrochromic device after applying potential +3V for 10s. (b) Photograph of colored state electrochromic device after applying a potential a of -3V for 10s. (c) Transmittance spectra for the electrochromic device in the colored and bleached states.

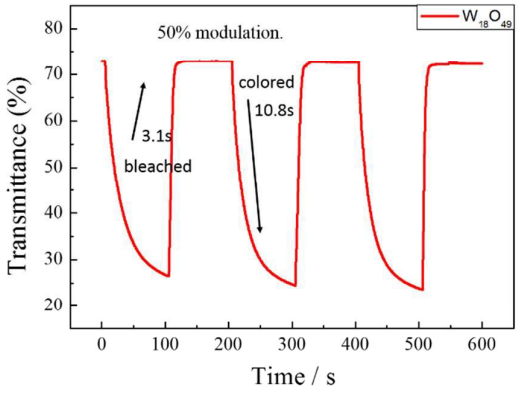

Fig.6 Switching time characteristics for $W_{18}O_{49}$ nanowire arrays film measured at -3 V to 3V at 632.8 nm.

Fig. 5(c) shows the measured transmittance spectra of the $W_{18}O_{49}$ nanowire arrays at +3.0 V and -3.0 V for 10s, respectively. It can be calculated that a contrast of 37.99% occurs at the wavelength of 632.8 nm. It is interesting to find that the $W_{18}O_{49}$ nanowire array films as the electrochromic layer shows a larger optical modulation above 404 nm, especially in the infrared region, which indicates a higher color contrast and larger heat regulation. However, most literatures reported the transmittance by using a wavelength of 632.8 nm as the judgement wavelength of tungsten oxide electrochromic films. For the purpose of comparison, the coloration/bleaching switching of the as-prepared non-stoichiometric tungsten oxide film was measured at 632.8 nm, as shown in fig. 6.

As revealed in the measurement, the WO_3 nanowire array films display a high contrast between the bleached (+3V) and colored states (-3V), and a more obvious change of transmittance can be found for increasing period of voltage application. The maximum optical modulation (ΔT%) of coloration/bleaching was found to be ~40.16% after applying a voltage for 100 s (-3V vs. +3V), which corresponds to the transmittance difference in fig. 5 (c). The coloration and bleaching times are extracted as the time required for 50% changes in the whole transmittance modulation at 632.8 nm. The coloration time and bleaching time for 50% transmittance changes are found to be 10.8 and 3.1 s, respectively. The switching response are faster than that of amorphous structures[34] and other traditional crystalline[35,36] WO_3, which indicates non-stoichiometric tungsten oxide nanowire film to be suitable for electrochromic devices. This phenomenon may be explained as follows: the $W_{18}O_{49}$ nanowires with smaller sizes stand vertically to the substrate, so they could offer a fast-path for ions and electrons which are inserted into or extracted from the host materials. Moreover, the deposited $W_{18}O_{49}$ nanowire with special tunnel structure provides shorter ionic diffusion paths into the lattice which facilitates the process of ion intercalation and deintercalation processes.

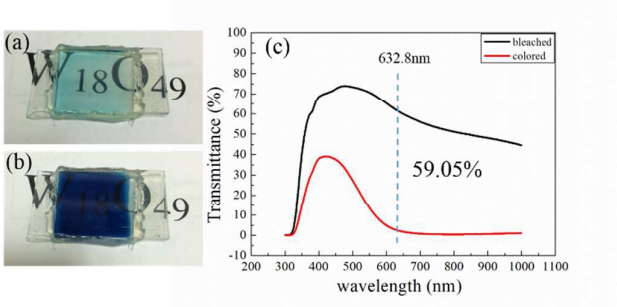

Fig.7 (a) Photograph of bleached state complementary electrochromic device after applying a potential of +3V for 10s. (b) Photograph of colored state electrochromic device after applying a potential of -3V for 10s. (c) Transmittance spectra for the electrochromic device in the colored and bleached states.

Compared with traditional monclinic WO_3 nanowire, WO_{3-x} nanowires exhibit strong absorption in near-infrared region (as shown in fig. 5 (c)), as reported to be owing to the abundant oxygen vacancies[37]. All the above reasons all explains that smaller sizes $W_{18}O_{49}$ nanowires can result in higher surface areas and provide more transport paths, which would be expected to have higher electrochromic layer-electrolyte contact areas and faster ion transport for achieving a superior electrochromic performance. To further improve the optical contrast and switching response time, the $W_{18}O_{49}$ nanowire arrays film is incorporated in an electrochromic device with an anodically colored Prussian blue film as a complementary electrochromic layer. Photographs of the complementary device are shown in fig. 7 (a,b), showing a high contrast between the bleached and colored states, which leads to obvious transmittance changes.

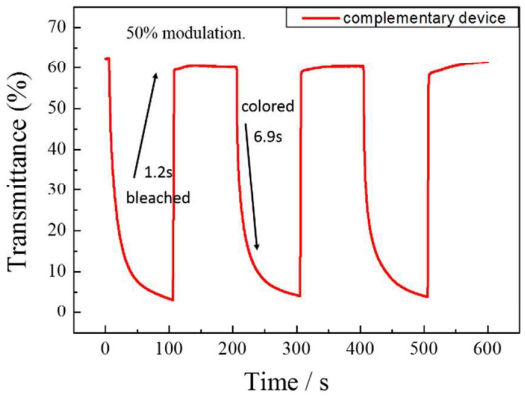

Fig.8 Switching time characteristics for $W_{18}O_{49}$ nanowire arrays film/Prussian blue measured at -3 V to 3V at 632.8 nm.

fig. 7(c) shows the measured transmittance spectra of the complementary device measured at +3.0 V and -3.0 V for 10 s, respectively. It can be calculated that a contrast of 59.05% occurs at the wavelength of 632.8 nm.

Fig. 8(a) shows the coloration/bleaching transmittance response of the complementary device measured at 632.8 nm. The maximum transmittance modulation (ΔT) of coloration/bleaching was found to be about 62.1% after applying a ±3.0 V voltage for 100 s, agreeing well with the transmitance spectra shown in fig. 7 (c). The coloration and bleaching times are extracted as the time required for 50% changes in the whole transmittance modulation at 632.8 nm. The coloration time and bleaching time for 50% transmittance changes are found to be 6.9 and 1.2 s, respectively. For the transmittance modulation of the electrochromic devices, the experimental data are summarized in Table S1. For the electrochromic devices using as-prepared $W_{18}O_{49}$ nanowire array film and complementary device structures, both the coloration/bleaching times for 50% and 90% modulation are faster than those previously reported[35,40]. The switching responses of the complementary device for both the coloration and bleaching processes demonstrate a better performance than that of single layer $W_{18}O_{49}$ nanowire arrays film or WO_3 nanowire arrays film, which is also much faster than similar studies

reported in the literatures[38,39]. the long-term cycling durability of the complementary device is also investigated and illustrated in Fig. S1. That is to say, it is expected that significant energy-saving can be realized by using the non-stoichiometric $W_{18}O_{49}$ nanowire arrays as electrochromic film in such kind of complementary devices.

Conclusions

In summary, non-stoichiometric $W_{18}O_{49}$ nanowire arrays were directly deposited on a seed-free FTO glass substrate by using an efficient and facile solvothermal method. It is shown that the solvothermal reaction time has a significant influence on the morphology of the as-prepared products. The results of XRD, FESEM, and TEM characterizations all evidenced the monoclinic phase to demonstrate good crystallinity and interwoven structure with large surface area. The $W_{18}O_{49}$ nanowire arrays exhibit high contrast and fast EC response time (coloring time~10.8s, bleaching time ~3.1s). In a complementary electrochromic device incorporating Prussian blue film as an anodically colored device, we obtained a larger optical contrast (59.05% at 632.8nm) and a faster switching response (coloring time ~6.9s, bleaching time ~1.2s), better than a single $W_{18}O_{49}$ nanowire film device. The complementary device can provide great promise for energy-saving smart windows and other related photoelectrical devices.

Acknowledgements

We acknowledge the financial support of the Ministry of Science and Technology (MOST), ROC grant through MOST 103-2221-E-006-089 and NSC 102-2221-E-024-003-MY3. Partial financial support from the Ministry of Economic Affairs, ROC is also acknowledged.

Notes and references

1. A. Georg and A. Georg, Sol. Energy Mater. Sol. Cells, 2009, 93, 1329.
2. S.J. Yoo, J.W. Lim, Y.E. Sung, Y.H. Jung, H.G. Choi and D.K. Kim, Appl. Phys. Lett., 2007, 90, 173126.
3. http://sageglass.com/technology/how-it-works/.
4. D. T. Gillaspie, R. C. Tenent, and A. C. Dillon, J. Mater. Chem., 2010, 20, 9585.
5. B. Xue, H. Li, L. Zhang and J. Peng, Thin Solid Films, 2010, 518, 6107.
6. S. Kim, M. Taya, and C. Xu, J. Electrochem. Soc., 2009, 156, E40.
7. G. A. Niklasson and C. G. Granqvist, J. Mater. Chem., 2007, 17, 127.
8. A.J. More, R.S. Patil, D.S. Dalavi, S.S. Mali, C.K. Hong, M.G. Gang, J.H. Kim and P.S. Patil, Mater. Lett., 2014, 134, 298.
9. C.H. Lu, M.H. Hon, C.Y. Kuan and I.C. Leu, Jpn. J. Appl. Phys., 2014, 53, 06JG08-1.
10. J. Wang, E. Khoo, P. S. Lee, and J. Ma, J. Phys. Chem. C, 2009, 113, 9655.
11. K.J. Patel, C.J. Panchal, M.S. Desai and P.K. Mehta, 2010, 124, 884.
12. J. Wang, E. Khoo, P. S. Lee, and J. Ma, J. Phys. Chem. C, 2008, 112, 14306.
13. J. Li, J. Zhu and X. Liu, New J. Chem., 2013, 37, 4241.
14. J. Zhang, J. P. Tu, G.H. Du, Z. M. Dong , Y. S. Wu, L. Chang, D. Xie, G. F. Cai and X. L.Wang, Sol. Energy Mater. Sol. Cells, 2013, 114, 31.
15. F. Zheng, H. Lu, M. Guo and M. Zhang, CrystEngComm, 2013, 15, 5828.
16. S. Y. Park, J. M. Lee, C. Noh and S. U. Son, J. Mater. Chem., 2009, 19, 7959.
17. V. V. Kondalkar, S. S. Mali, R. R. Kharade, K. V. Khot, P. B. Patil, R. M. Mane, S. Choudhury, P. S. Patil, Dalton Trans., 2015, 44, 2788.
18. J. Zhang, J. P. Tu, X. H. Xia, X. Li Wang and C. D. Gu, J. Mater. Chem., 2011, 21, 5492.
19. S. Zhuiykov and E. Kats, Nanoscale Res. Lett., 2014, 9, 401.
20. V. Madhavi, P. Kondaiah, O. M. Hussain and S. Uthanna, Physica B, 2014, 454, 141.
21. J. Denayer, P. Aubry, G. Bister, G. Spronck, P. Colson, B. Vertruyen, V. Lardot, F. Cambier, C. Henrist and R. Cloots, Sol. Energy Mater. Sol. Cells, 2014, 130, 623.
22. J. R. G. Navarro, A. Mayence, J. Andrade, F. Lerouge, F. Chaput, P. Oleynikov, L. Bergstrom, S. Parola and A. Pawlicka, Langmuir, 2014, 30 ,10487.
23. V.V. Kondalkar, R.R. Kharade, S.S. Mali, R.M. Mane, P.B. Patil, P.S. Patil, S. Choudhury and P.N. Bhosale, Superlattices Microstruct., 2014, 73, 290.
24. G. F. Cai, J. P. Tu, D. Zhou, X. L. Wang, C. D. Gu, Sol. Energy Mater. Sol. Cells, 2014, 124, 103.
25. M. Wu, X. Lin, L. Wang, W. Guo, Y. Wang, J. Xiao, A. Hagfeldt and T. Ma, J. Phys. Chem. C, 2011, 115, 22598.
26. Y. T. Hsieh, U. S. Chen, S. H. Hsueh, M. W. Huang and H. C. Shih, Appl. Surf. Sci., 2011, 257, 3504.
27. K. Huang, Q. Pan, F. Yang, S. Ni and D. He, Appl. Surf. Sci., 2007, 253, 8923.
28. Y. Qin, X. Li, F. Wang and M. Hu, J. Alloy. Compd., 2011, 509, 8401.
29. J. Liu, S. Yu, W. Zhu and X. Yan, Applied Catalysis A: General, 2015, 500, 30.
30. A. Danine, L. Cojocaru, C. Faure, C. Olivier, T. Toupance, G. Campet, A. Rougier, Electrochim. Acta, 2014, 129, 113.
31. Z. Lou, Q. Gu, L. Xu, Y. Liao, and C. Xue, Chem. Asian J., 2015, 10, 1291.
32. H. Zhou, Y. Shi, Q. Dong, Y. Wang, C. Zhu, L. Wang, N. Wang, Y. Wei, S. Tao and T. Ma, J. Mater. Chem. A, 2014, 2, 4347.
33. X. Chang, S. Sun, Z. Li, X. Xu and Y. Qiu, Appl. Surf. Sci., 2011, 257, 5726.
34. D. Chatzikyriakou, N. Krins, B. Gilbert, P. Colson, J. Dewalque, J. Denayer, R. Cloots and C. Henrist, Electrochim. Acta, 2014, 137, 75.
35. J. Wang, E. Khoo, P. S. Lee and J. Ma, J. Phys. Chem. C, 2008, 112, 14306.
36. H. Qu, X. Zhang, L. Pan, Z. Gao, L. Ma, J. Zhao, Y. Li, Electrochim. Acta, 2014, 148, 46.
37. G. Xi, S. Ouyang, P. Li, J. Ye, Q. Ma, N. Su, H. Bai and C. Wang, Angew Chem Int Edit, 2012, 51, 2395.
38. Z. Jiao, J. Wang, L. Ke, X. Liu, H. V. Demir, M. F. Yang, X. W. Sun, Electrochim. Acta, 2012, 63, 153.
39. F. Zheng, H. Lu, M. Guo and M. Zhang, CrystEngComm, 2013, 15, 5828.
40. Z. Jiao, X. W. Sun, J. Wang, L. Ke and H. V. Demir, J. Phys. D: Appl. Phys., 2010, 43, 285501.